

ON FLUID-DRIVEN CRACK PROPAGATION ALONG BIMATERIAL INTERFACES

Xi Zhang & Rob Jeffrey

CSIRO Petroleum, Ian Wark Laboratory, Bayview Avenue, Clayton, VIC 3168, Australia.

ABSTRACT

The problem of growth of a hydraulic fracture located at the interface between two impermeable linearly elastic solids is considered. An incompressible Newtonian fluid is supplied at a constant injection rate into the crack to promote crack propagation. The energy release rate criterion is adopted to control crack growth. A hybrid scheme of Displacement Discontinuity Method and Finite Difference Method is employed to solve the nonlocal and nonlinear coupled problem. Numerical results are obtained to examine the effects of the contrast of Young's modulus, the fluid viscosity and the confining stress, on the fracture growth rates, the stress and opening profiles. The possibility of the fluid front not reaching the crack tip can result in a fluid lag zone, which is taken into account in the numerical method.

1. INTRODUCTION

The hydraulic fracturing technique has been widely used for oil and gas stimulation, geothermal reservoir stimulation, and drilling waste disposal. In layered sedimentary rocks, the fractures have been observed to deviate into a relatively weak bedding plane and to cause local opening along the contact plane (Cooke and Underwood[1]). Layered rock systems, such as coal and sandstone, can exhibit a strong contrast in stress and Young's modulus across the layer interfaces. There is a need to better understand the fracture behavior of fluid-driven interfacial crack for hydraulic fracture growth along such interfaces for application to fracture prediction and design.

Interfacial crack problems have received considerable attention in the past decade. However, there are no existing solutions for the fluid-driven cracks along an interface although the early work by Williams [2] is geology-related. He found that for cracks along on an interface between two elastic materials, there are predicted nonphysical stress oscillation and material interpenetration very close to the crack tip. However, the more widely used approach in engineering applications follows the concept of small-scale contact presented by Rice [3] which ignore this aspect of the solution.

Fractures can propagate without the fluid completely filling the fracture. In this case, there is a fluid lag zone between the fluid front and the crack tip. The existence of the lag zone affects the crack opening and fluid pressure and, therefore, the crack growth rates. The lag zone size may vary with time and is sensitive to the far-field stress states. It is of interest to study the role of elastic modulus and far-field stress contrasts on the lag zone size for an interfacial crack.

We use numerical experiments to investigate the mechanism of fluid-driven crack propagation along an interface between two elastic solids. The crack problem is formulated in Section 2. An incompressible Newtonian fluid is injected at a constant injection rate into the crack to promote crack propagation. The energy release rate is adopted for the crack growth criterion. A hybrid scheme of Displacement Discontinuity Method and Finite Difference Method described in Section 3 is employed to solve the nonlocal and nonlinear coupled problem.. Numerical results are given in Section 4 to examine the effects of the contrast of Young's modulus, fluid viscosity and the confining stress, on the fracture growth rates, pressure and opening profiles.

2. PROBLEM FORMULATION

Consider quasi-static crack advance along an interface between two elastic solids, as shown in

Fig.1. The half crack length at time t is $a(t)$ and the fluid-filled length is $b(t)$. Young's modulus, shear modulus and Poisson's ratio above and below the interface are denoted by E_1, μ_1, ν_1 and E_2, μ_2, ν_2 , respectively. In the absence of body force, the equilibrium equation for interfacial cracks is

$$\beta \delta'(x) + \int_{-a}^a \frac{\delta(s, t)}{(x-s)^2} ds = \frac{1}{C} [p(x) - \sigma_0] \quad (1)$$

$$\int_{-a}^a \frac{\delta(s, t)}{(x-s)^2} ds + \beta \omega'(x) = 0$$

in which Dundur's mismatch parameters are defined as

$$\alpha = \frac{\mu_1(\kappa_2 + 1) - \mu_2(\kappa_1 + 1)}{\mu_1(\kappa_2 + 1) + \mu_2(\kappa_1 + 1)} \quad (2)$$

$$\beta = \frac{\mu_1(\kappa_2 - 1) - \mu_2(\kappa_1 - 1)}{\mu_1(\kappa_2 + 1) - \mu_2(\kappa_1 + 1)}$$

where $\kappa_i = 3 - 4\nu_i$; and C is the effective bi-material modulus

$$C = \frac{2\mu_1(1 + \alpha)}{(\kappa_1 - 1)(1 - \beta^2)} \quad (3)$$

The discontinuities in the normal and tangential directions are denoted by ω and δ , respectively. And $p(x)$ is the internal fluid pressure and σ_0 is the confining stress across the interface.

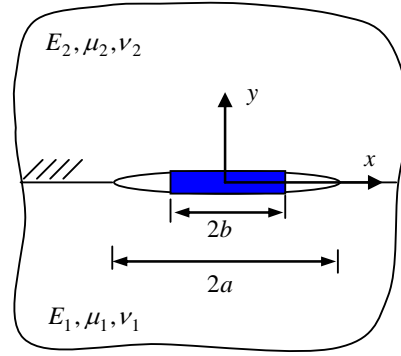


Fig. 1 The fluid-driven interfacial crack problem

With regard to fluid filled region $[-b, b]$, the fluid is assumed to be an incompressible, Newtonian fluid. The lubrication equation is valid in this case. Thus, we have

$$\frac{\partial \omega}{\partial t} = -\frac{\partial}{\partial x} \left(\frac{\omega^3}{12\eta} \frac{\partial p}{\partial x} \right) \quad (4)$$

in which η is the fluid dynamic viscosity.

The injection condition is taken as the constant injection rate, Q_0 , that is,

$$q(0,t) = Q_0/2 \quad (5)$$

Which accounts for the fact that the total flow is divided between the two symmetric sides of the crack. The global mass balance requires

$$\int_{-b}^b \omega(x,t) dx = Q_0 t \quad (6)$$

The vanishing opening and shearing at the crack tip implies

$$\omega(a,t) = 0 \quad \delta(a,t) = 0 \quad (7)$$

Ahead of the tip of the interfacial crack, there is a singular stress field which can be expressed as

$$\sigma_{22} + i\sigma_{12} = \lim_{r \rightarrow 0} \frac{K_1 + iK_2}{\sqrt{2\pi r}} \left(\frac{r}{a}\right)^{i\varepsilon} \quad (8)$$

in which $r = a - x$, $\varepsilon = 1/2\pi \ln[(1-\beta)/(1+\beta)]$ and K_i is the complex stress intensity factor. Instead of calculating K_i , a maximum Energy Release Rate, Γ , criterion is used for crack propagation, see Geubelle and Knauss [4]. Their expressed for Γ in terms of opening and sliding displacements is as follows

$$\Gamma = \frac{\pi(1+4\varepsilon^2)}{8[(1-\nu_1)/\mu_1 + (1-\nu_2)/\mu_2]} \lim_{r \rightarrow 0} \frac{\omega^2 + \delta^2}{r} \quad (9)$$

3. NUMERICAL METHOD

An adaptive-mesh scheme is employed for solving the boundary-value problems in the previous section. Two sizes of constant displacement discontinuity elements are used, based on the element location. The element size of coarse elements is three times of the fine elements. The first six elements adjacent to the crack tip are always of fine element size, while others are coarse elements. The tip element has a square-root singularity in displacement discontinuities. With crack propagation, one normal element size is added to the crack. The newly-created crack surface is discretized by the fine elements. To limit the overall number of fine elements, the three fine elements furthest from the tip must be changed to one coarse element.

The hypersingular elasticity equation, Eq. (1), is solved by the ordinary Displacement Discontinuity Method (DDM) with unknown internal fluid pressure. The fluid flow in the hydraulic fractures is solved through Finite Difference Method (FDM) with a discretization in time. An implicit scheme is used to seek a convergent solution after a small time increment Δt . The solution method accounts for the fact that the crack can be only partially filled with fluid. The lubrication equation for fluid flow in element i can be rewritten as

$$\frac{\Omega_i^{r+1} - \Omega_i^0}{\Delta t} = \frac{1}{\Delta \xi^2} [\alpha_{out} (\Pi_{i+1}^{r+1} - \Pi_i^{r+1}) - \alpha_{in} (\Pi_i^{r+1} - \Pi_{i-1}^{r+1})] \quad (10)$$

in which $r+1$ is the iteration step and Ω, Π, ξ and t are normalized opening, fluid pressure, coordinate and time, (see Zhang et al.[5]). The expressions for two coefficients are

$$\alpha_{out} = \left(\frac{\Omega_{i+1}^r + \Omega_i^r}{2}\right)^3 \quad (11)$$

$$\alpha_{in} = \left(\frac{\Omega_i^r + \Omega_{i-1}^r}{2}\right)^3$$

The crack opening can be obtained by checking the relative error after each iteration step to insure that a convergence tolerance is met. After the convergent opening is obtained, the location of the fluid front can be calculated by the mass balance in the filling elements. Through algebraic manipulations (see Zhang et al. [5]), the ratio ϕ of fluid-filled length in the filling element to the element size is found to be

$$\phi = \frac{\Delta t}{\Delta \xi} \frac{\Psi_{M+1/2}}{\Omega_{M+1}} \quad (12)$$

in which the flux into the filling element M is

$$\Psi_{M+1/2} = \left(\frac{\Omega_M + \Omega_{M+1}}{2} \right)^3 \frac{\Pi_M - \Pi_{M+1}}{\Delta \xi} \quad (13)$$

4. NUMERICAL RESULTS

In this section, the following material constants are specified: $E_1 = 10000$ MPa, $\nu_1 = \nu_2 = 0.25$ and $\Gamma = 100$ N/m. An injection rate, $Q_0 = 0.0001 \text{ m}^2 / \text{s}$, is used for all cases. To evaluate the effects of Young's modulus contrast, the variations of crack length and lag size in time are displayed in Fig. 2 for various modulus contrasts using $\eta = 0.1 \text{ Pa.s}$ and $\sigma_0 = 2$ MPa. The crack speed decreases in time, as does the lag size. It is found that with decreasing the Young's modulus in material 2, the crack growth rate decreases. The lag size is also reduced by increasing the contrast E_1 / E_2 . At larger contrasts, there is no lag zone

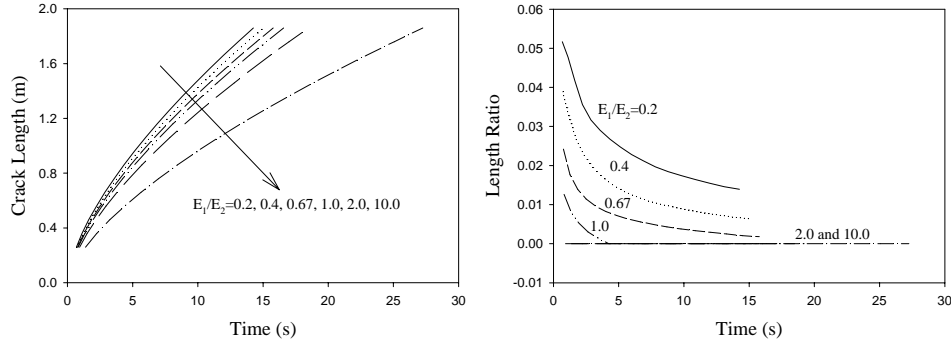


Figure 2: Time dependence of crack length and length ratio for various values of E_1 / E_2 .

Figure 3 show the variations of crack length and lag size in time for different values of fluid viscosity at $E_2 = 50000$ MPa and $\sigma_0 = 2$ MPa. It is seen from Fig. 3 that if the injection rate is fixed, the crack growth rate decreases with increasing viscosity. On the other hand, there is a large lag zone at large viscosities and no lag can be detected if $\eta = 0.001$ Pa.s.

The effect of the confining stresses on crack growth rate and lag size is depicted in Fig. 4 at $E_2 = 50000$ MPa and $\eta = 0.1 \text{ Pa.s}$. It is found that with increasing confining stress, the crack growth rate is reduced and the lag size decreases. For the case of vanishing confining stresses, the lag size is constant, while the lag size decreases in time at non-zero confining stresses.

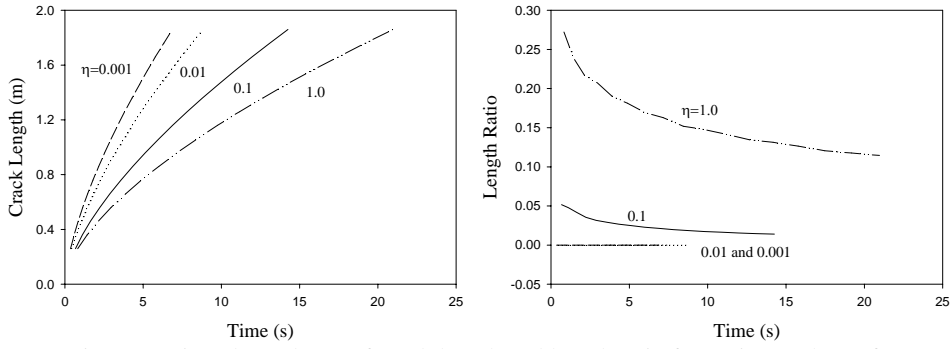


Figure 3: Time dependence of crack length and length ratio for various values of η .

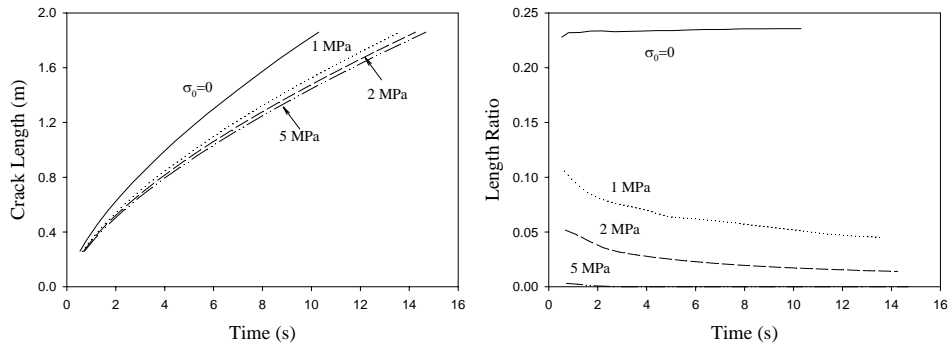


Figure 4: Time dependence of crack length and length ratio for various values of σ_0 .

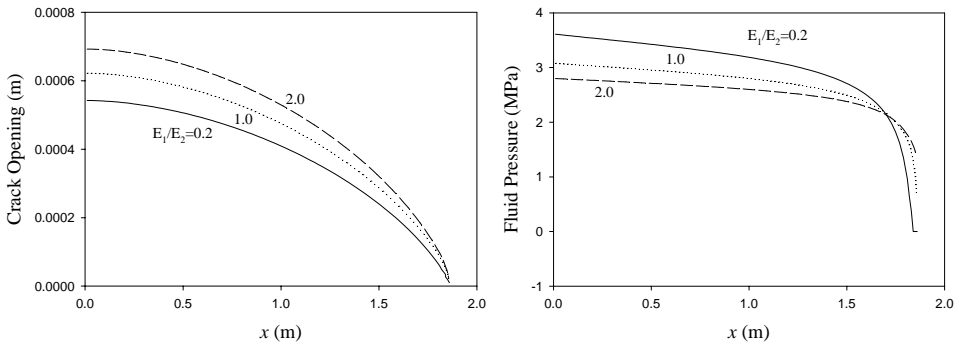


Figure 5: Distribution of crack opening and fluid pressure along the crack for various values of E_1 / E_2 at the specified half crack length $a(t) = 1.86\text{m}$.

The profiles of crack opening and fluid pressure at a specified crack length are plotted in Fig. 5 for different contrasts for $\eta = 0.1 \text{ Pa}\cdot\text{s}$ and $\sigma_0 = 2 \text{ MPa}$. It is found that the opening depends on the average Young's modulus $(E_1 + E_2)/2$. A small fluid lag zone can be seen in Fig. 5 for the case of $E_1 / E_2 = 2$ as a region with zero fluid pressure. The fluid pressure gradient increases near the crack tip as the Young's modulus of material 2 is increased, reflecting the overall decrease in the opening and the associated increase in viscous losses.

5. CONCLUSIONS

In this paper, fluid-driven crack propagation along an interface between two elastic solids is studied numerically. Numerical results are provided for the effects of the contrast of Young's modulus, fluid viscosity and confining stress, on the fracture growth rates, pressure and opening profiles. It is found that these factors affect the crack growth rate and the fluid lag size, as well as the distributions of opening and fluid pressure.

REFERENCES

- [1] Cooke, M. L. and Underwood, C. A. Fracture termination and step-over at bedding interfaces due to frictional slip and interface opening, *J. of Structural Geology* 23, 223-238, 2001.
- [2] Williams, M. L. The stress around a fault or crack in dissimilar media, *Bulletin of the Seismological Society of America* 49, 199-204, 1959.
- [3] Rice, J. R. Elastic fracture mechanics concepts for interfacial cracks, *J. Appl. Mech.* 55, 98-103, 1988.
- [4] Geubelle, P. H. and Knauss, W. G. Crack propagation at and near bimaterial interfaces: linear analysis, *J. Appl. Mech.* 61, 560-566, 1994.
- [5] Zhang, X., Detournay, E. and Jeffrey, R. Propagation of a penny-shaped hydraulic fracture parallel to the free-surface of an elastic half-plane, *Int. Jour. of Fracture.* 115, 125-158, 2002.